Veterinary Oncology

RESEARCH

Open Access

Correlation between microvascular density and perfusion parameters derived from dynamic contrast-enhanced computed tomography in dogs with tumors of the head

Jeremy R. Mortier[1,3,4*], Peter Richards-Rios[2], Lorenzo Ressel[2] and Valeria Busoni[3]

Abstract

Background Non-resectable tumors of the head can represent a therapeutic challenge in dogs and prognostic indicators and markers of response to treatment are needed. Tumor microenvironment, in particular microvascular density (MVD), affects response to treatment and prognosis.

Methods Perfusion parameters obtained from dynamic contrast-enhanced computed tomography (DCECT) have been correlated to MVD and outcome in humans. Twenty-five dogs comprising 16 epithelial tumors and 9 mesenchymal tumors of the head were prospectively recruited and underwent DCECT. Microvascular density (anti-Factor VIII) was assessed using a trained object classifier in stroma and tumor tissue.

Results Mesenchymal tumors had significantly higher percentage area of blood vessels in tumor tissue than epithelial tumors ($P = .04$). There was no significant association between perfusion parameters and MVD measurements.

Conclusions These findings suggest that mesenchymal tumors have a higher MVD than epithelial tumors, and that perfusion parameters derived from DCECT might not be well correlated with MVD in dogs with tumors of the head.

Keywords DCECT, Perfusion, Microvascular density, Dogs, Neoplasms, Head

Background

Tumors originating from the nasal cavities and from the bones and soft tissues of the face in dogs can represent a therapeutic challenge due to their poor surgical resectability and the morbidity associated with surgery [1, 2].

There is increasing evidence that tumor microenvironment, and in particular the microvascular density (MVD), has important influence on the prognosis of various tumor types, both in humans and animals [3–12]. Epithelial and mesenchymal tumors have different microenvironments that could have an impact on response to treatment and could explain why canine nasal carcinomas show a greater decrease in size after radiotherapy (RT) than canine nasal sarcomas, even though survival

*Correspondence:
Jeremy R. Mortier
jeremy.mortier@vet-alfort.fr
[1] Small Animal Teaching Hospital, Institute of Infection, Veterinary and Ecological Sciences, University of Liverpool, Neston, UK
[2] Department of Veterinary Anatomy, Physiology and Pathology, Institute of Infection, Veterinary and Ecological Sciences, University of Liverpool, Neston, UK
[3] Diagnostic Imaging Section, Department of Clinical Sciences, Faculty of Veterinary Medicine, University of Liège, Liège, Belgium
[4] Present address: Service d'imagerie médicale (ChuvAC), DEPEC, École Nationale Vétérinaire d'Alfort, 7 avenue du Général de Gaulle, 94700 Maisons-Alfort, France

times were not significantly different between tumor types [13, 14].

Dynamic contrast-enhanced computed tomography (DCECT) is a non-invasive technique measuring perfusion parameters of a chosen area through temporal changes in attenuation after intravenous injection of iodinated contrast medium [15]. These parameters classically include blood volume (BV), blood flow (BF) and transit time (TT). In human medicine, DCECT has shown promise as a prognostic indicator and is used to assess response to treatment and to detect local recurrence [16–19]. It was also shown that canine sarcomas had lower perfusion parameters than canine carcinomas, and no association was found between perfusion parameters and survival in canine nasal tumors [20–22].

In human medicine, several studies on various types of tumors including head and neck squamous cell carcinoma, prostatic neoplasia, pancreatic endocrine tumors and pancreatic carcinoma, have shown positive correlations between the perfusion parameters derived from DCECT and MVD [23–25]. However, perfusion parameters have never been correlated with MVD in spontaneous canine tumors.

The objectives of our study were (1) to compare the perfusion parameters derived from DCECT and the MVD in a group of dogs with tumors of the head and (2) to compare MVD between epithelial and mesenchymal tumors. Our hypotheses were that there would be a positive correlation between the perfusion parameters and the MVD and that epithelial and mesenchymal tumors would have different MVD.

Methods

Experimental design

This is a prospective cross-sectional study.

Case selection

Client-own dogs presented to the Small Animal Teaching Hospital of the University of Liverpool for suspicion of tumors originating from the nasal cavities or facial bones and soft tissues were prospectively enrolled from January 2017 to January 2020. Owner consent allowing for diagnostic tests including DCECT was obtained before inclusion into the study. Ethics approval was granted by the Veterinary Research Ethics Committee of the University of Liverpool under the reference VREC560a. To meet the inclusion criteria, a histological diagnosis of neoplasia was required, and dogs must have undergone at least a baseline DCECT. Dogs who had already received RT, tyrosine kinase inhibitors, chemotherapy, and dogs who had prior surgery for their tumor were excluded. Dogs receiving other non-chemotherapeutic medical treatments for their tumor (anti-inflammatory and antimicrobial medications) and dogs who had surgical biopsy of their tumor performed were not excluded.

Clinical data

Histological tumor types were determined on biopsy samples by board-certified pathologists and classified as epithelial (squamous cell carcinoma, transitional cell carcinoma, adenocarcinoma, undifferentiated carcinoma, acanthomatous ameloblastoma) or mesenchymal (fibrosarcoma, chondrosarcoma, hemangiosarcoma, undifferentiated sarcoma). Biopsies from nasal tumors were performed under endoscopic guidance, whereas biopsies from tumors of the mandible and maxilla were surgically performed.

Immunostaining

Sections of tissue fixed in 4% paraformaldehyde solution underwent tissue processing using a Tissue-Tek vacuum infiltration processor (VIP) overnight before being embedded in paraffin (Ultraplast premium embedding medium, Solmedia). Paraffin sections of 4 µm were cut on a Leica RM2125 RT microtome. Slides were stained using standard hematoxylin and eosin H&E staining techniques.

Immunostaining was performed on a Dako Autostainer Link 48 using Envision FLEX reagents.

Following a buffer rinse, tissue sections underwent a peroxidase block for 5 min (Agilent, SM801) before being incubated for 20 min with mouse monoclonal antibodies against mammalian Factor VIII antigens (Agilent, A0082). The Factor VIII (1:2000) antibodies were diluted in Envision FLEX antibody diluent (Agilent, K8006). Antibody binding was detected using the labelled polymer Envision FLEX/HRP (Agilent, SM802) for 20 min, and the reaction was visualized using the substrate-chromogen FLEX 3,3′-Diaminobenzidine (DAB) + SubChromo (Agilent, DM827 and SM802). Tissue sections were counter-stained for 5 min in Envision FLEX hematoxylin (Agilent, K8008), washed in deionized water, and dehydrated through increasing grades of ethanol (85%, 96%, 3 X 100%) before clearing in xylene and mounted. All intermediate buffer washes between reagents used Envision FLEX wash buffer (K8007).

Measurement of microvascular density (MVD)

Examination and analysis of the slides was conducted by a European College of Veterinary Pathology resident (PR) under the supervision of a European College of Veterinary Pathology board-certified veterinary pathologist (LR). Hematoxylin and eosin and DAB immunostained slides were scanned at 40X magnification using an Aperio slide scanner. Digital slides were examined using QuPath v0.2.3 [26]. An object classifier to detect blood

vessels based on DAB-positive staining was trained on representative sections of tumor and stroma from 13 slides. To improve sensitivity, areas of likely false positivity such as fibrin clots and epithelium were excluded from representative sections. 3,3′-Diaminobenzidine positive cell detection was conducted on the optical density sum image using default settings with the exception of background radius which was set at 4 µm. The intensity threshold parameters were assessed on the cell mean with threshold positivity set at 0.035.

Smoothed features for each detection with a radius of 25 µm were added using the "Smooth object features" command. Tissue within representative sections was manually annotated as either “blood vessel” or “not blood vessel”. A Random trees object classifier was then trained on detections and annotations. The accuracy of the object classifier was assessed on a testing set of 5 slides. Representative sections of tumor and stroma were selected, DAB positive cell detection and adding of smoothed features were conducted as for training slides. Test slides were duplicated along with detections and annotations, with one copy manually annotated for presence of blood vessels and the object classifier applied to the other. Detection features were exported from the manually annotated and object classifier copies of test slides and compared to determine the object classifier's specificity and sensitivity.

For comparing the prevalence of blood vessels in epithelial and mesenchymal tumors, DAB-stained slides were examined. All contiguous tissue on the slide was annotated as either tumor or stroma based on histologic appearance. An area was annotated as tumor if it was composed of neoplastic cells and tumor stroma. An area was annotated as stroma if it was composed of normal connective tissue and contained no neoplastic cells or epithelium. Areas of high false positive DAB staining were excluded from annotated areas. DAB positive cell detection and addition of smoothed features were carried out as previously described before the object classifier was applied to the annotations. Measurements of detections from all slides were exported including object classifications (blood vessel or not blood vessel), parent annotation (tumor or stroma) and cell area (Fig. 1).

Data was processed in Python using pandas v0.25.3 [27] to calculate the total number of detections and cell area in tumor and stroma annotations and subsequently the percentage detections (PctBVeTum and PctBVeStrom in tumor tissue and stroma, respectively) and cell area (PctAreaBVeTum and PctAreaBVeStrom in tumor tissue and stroma, respectively) that was classified as BV by the object classifier.

Dynamic contrast-enhanced computed tomography (DCECT)

All dogs were premedicated with medetomidine (0.003 to 0.01 mg/kg) in association with butorphanol, buprenorphine or methadone. Anesthesia was induced using propofol or alfaxolone (to effect) and maintained using sevoflurane. Dynamic contrast-enhanced CT was performed using an 80-slice CT scan (Aquilion Prime 80, Canon Medical System) with dogs in sternal or dorsal recumbency depending on the location of the mass.

A pre-contrast CT scan of the head was acquired. Scanning parameters were 120 kV, variable mAs using Automatic Exposure Control, pitch factor 0.625, and images were reconstructed at 1 mm slice thickness using bone and soft tissue reconstruction algorithms. Dynamic contrast-enhanced CT planning was done using the pre-contrast soft tissue reconstruction in a soft tissue window (window width 200 HU, window level 40 HU). A 4-cm length field of view was chosen to include the entirety of the tumor or the tumor center if the total mass was longer than 4 cm. For DCECT, a 60-s continuous scan starting with intravenous injection of 2 mL/kg body weight of

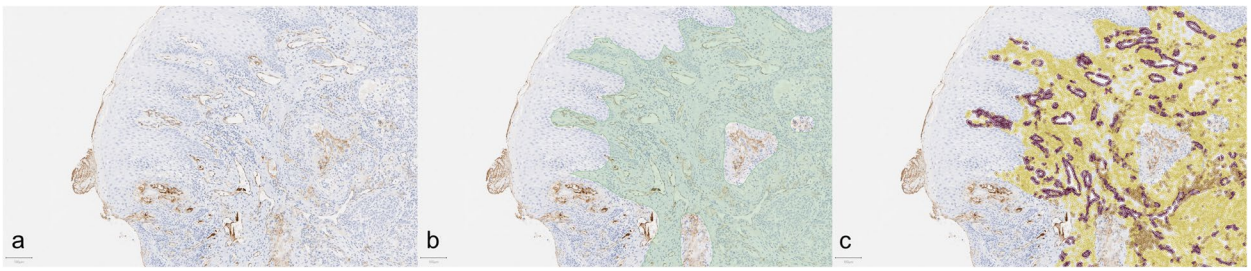

Fig. 1 Photomicrographs showing selective annotation and cell detections classified as either blood vessel (BV) or not blood vessel (NBV). **a** A DAB-stained section showing hyperplastic epithelium overlying stroma. **b** The area highlighted in green was annotated as stroma for analysis. The epithelium and sections of stroma with large areas of false positive DAB staining were excluded from the analysis. **c** Cell detections are colored as to whether they have been identified as DAB positive (dark coloration) or negative (light coloration) and identified by the classifier as BV (maroon) or NBV (yellow)

iodinated contrast medium (Ioversol 300 mg/mL iodine) using a power injector set at 3 mL/s injection rate (maximal allowable injection pressure set at 150 psi) and followed by a bolus flush of saline 1 mL/kg at the same injection rate was performed. Scanning parameters were 80 kV, 200 mA, 0.75 s rotation time, 0.5 mm scan slice thickness, 1 s time interval and 2 mm reconstruction slice thickness. Images were reconstructed using a soft tissue reconstruction algorithm. Dynamic contrast-enhanced CT was followed by a delayed post-contrast acquisition using the same parameters as the pre-contrast acquisition. Tumor volume was calculated on the post-contrast soft tissue reconstruction using multiplanar reconstruction and the ellipsoid formula $V = 4/3 \times \pi \times L \times W \times H$.

Perfusion analysis

Dynamic contrast-enhanced computed tomographic images were analyzed using an adiabatic approximation to the tissue homogeneity (ATH) model implemented with MATLAB™ (MathWorks, Massachusetts) [28]. An arterial input function was first contoured, and a time-attenuation curve displayed to verify it had a shape consistent with arterial blood flow. The artery selected for the arterial input function was the deep lingual artery as it was consistently the largest artery included in the field of view not surrounded with bone. To appropriately contour the artery without selecting peripheral lingual tissue the image was zoomed in and contoured on the arterial phase (veins not contrast-enhanced). Only the center of the artery was included when possible. The mass was then contoured manually slice by slice on every slice containing suspected tumoral tissue (Fig. 2). Care was taken not to include bone within the contouring. Perfusion parameters obtained from the analysis were blood flow (BF) and transit time (TT). Fractional vascular fraction (blood volume, BV) could then be calculated using the following formula: $BV = TT \times BF$. Perfusion analysis was performed by one trained operator (JM). Perfusion parameters of the nasal tumors and orofacial tumors included in this study were previously described by the authors. [21, 22].

Statistical analysis

All statistical tests were selected and performed by a statistician using R (version 3.6.2, The R Foundation for Statistical Computing). All dependent and independent variables were derived from the clinical data, CT examinations and histopathological examinations. Descriptive

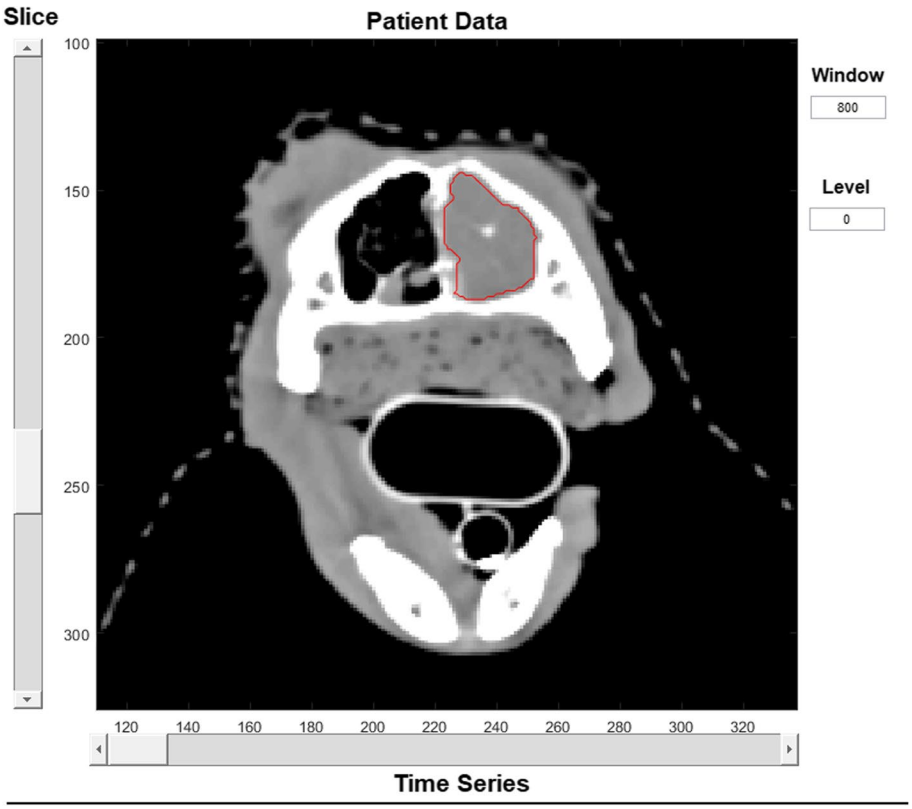

Fig. 2 Computed tomographic image of a nasal tumor in transverse plane and soft tissue window using the perfusion analysis software and showing the contouring of the mass (red line) for subsequent perfusion analysis. x-axis and y-axis are the time series and CT slices, respectively

statistics were calculated for data where appropriate; categorical variables were summarized as frequencies with 95% confidence intervals (CI) and continuous variables as means and standard deviations or medians with interquartile ranges (IQR). The distribution of any continuous variable was assessed for deviation from normal distribution with the Shapiro-Wilk test.

Multiple regression analysis was carried out to identify existing relationships between the variables BV, BF, TT, tumor volume and histological group and the variables PctBVeTum, PctAreaBVeTum, PctBVeStrom and PctAreaBVeStrom.

In a second time, a Levene test was carried out to test equality of variances between the two groups (epithelial tumors VS mesenchymal tumors) and one-sided Student T-tests were used to analyze mean differences between the normal continuous variables (BV, BF, TT, PctBVeTum, PctAreaBVeTum, PctBVeStrom and PctAreaBVeStrom). *P*-values < 0.05 were considered significant.

Results

Clinical data

Twenty-five dogs met the inclusion criteria. Median age was 9.5 years (1.5-12.8); median weight was 20.7 kg (5.9-54). There were 4 crossbreeds, 3 Labradors, 2 border collies and 1 of each of the following breeds: rottweiler, West Highland white terrier, pug, Rhodesian ridgeback, Jack Russel terrier, Yorkshire terrier, Airedale terrier, cocker Spaniel, Airedale terrier, Irish setter, lurcher, border terrier, Cairn terrier, English springer terrier, boxer and beagle. Twelve dogs were spayed females, 7 were castrated males, 4 were intact males and 2 were intact females.

There were 16 epithelial tumors and 9 mesenchymal tumors. Epithelial tumors included 5 carcinomas, 4 squamous cell carcinomas, 3 transitional carcinomas, 3 adenocarcinomas, and 1 acanthomatous ameloblastoma. Mesenchymal tumors included 5 chondrosarcomas, 2 poorly differentiated sarcomas, 1 fibrosarcoma, and 1 hemangiosarcoma.

Seventeen dogs had a tumor originating from the nasal cavity (5 carcinomas, 5 chondrosarcomas, 3 adenocarcinomas, 3 transitional carcinomas, 1 hemangiosarcoma), 3 had a tumor centered on the palatine bone (2 poorly differentiated sarcomas, 1 squamous cell carcinoma), 2 had a tumor centered on the maxillary bone (1 fibrosarcoma, 1 squamous cell carcinoma), 2 had a tumor centered on the mandible (both squamous cell carcinomas), and 1 had a tumor centered on the incisive bone (acanthomatous ameloblastoma).

At presentation, 6 dogs were receiving NSAID, 3 dogs were receiving a treatment classified as "other" (trimethoprim-sulfamethoxazole in 1 dog, amoxicillin-clavulanate in 1 dog, and vitamin K1 in 1 dog), 2 dogs were receiving corticosteroids and 14 dogs had no treatment at the time of presentation.

In total, 19/25 dogs had a record of their heart rate during the baseline DCECT, at the time of injection of contrast medium. All were considered appropriate by the attending anesthetist and ranged from 40 to 130 bpm (median 85 bpm). Similarly, systolic blood pressure was obtained for 13 dogs and ranged from 80 to 130 mmHg (median 100 mmHg).

Dynamic contrast-enhanced computed-tomography

Fifteen dogs had a tumor with a length greater then 4 cm (9 epithelial tumors, 6 mesenchymal tumors). Median volume for epithelial tumors and for mesenchymal tumors were 108.3 cm^3 and 150.8 cm^3, respectively.

Perfusion parameters for epithelial and mesenchymal tumors are shown in Table 1. Median BV, BF and TT for the epithelial tumors were 17.8 (3-66) mL/100 g, 132.1 (48–274.2) mL/100 g/min, and 7 (4.1-14.2) s. Median BV, BF and TT for the mesenchymal tumors were 8.1 (2.5-18.3) mL/100 g, 59.9 (3.8-121.6) mL/100 g/min, and 9.5 (4.5-49.6) s.

Microvascular density

All tumors were annotated for tumor and stroma tissue yielding 11 annotations of epithelial tumor associated stroma, 12 annotations of epithelial tumor, 7 annotations of mesenchymal tumor and 5 annotations of mesenchymal tumor associated stroma for cell detection. Parameters of MVD for epithelial and mesenchymal tumors are shown in Table 2.

Median PctBVeTum, PctAreaBVeTum, PctBVeStrom and PctAreaBVeStrom for epithelial tumors were 2.3% (0.4-4.5%), 2.8% (0.6-4.1%), 11.2% (5.2-22.6%), and 12% (4.7-22%).

Median PctBVeTum, PctAreaBVeTum, PctBVeStrom and PctAreaBVeStrom for mesenchymal tumors were

Table 1 Median blood volume (BV), blood flow (BF) and transit time (TT) derived from dynamic contrast-enhanced computed tomography in 16 dogs with an epithelial tumor and 9 dogs with a mesenchymal tumor of the head

	Median BV (range) (mL/100 g)	Median BF (range) (mL/100 g/min)	Median TT (range) (s)
Epithelial tumors	17.8 (3-66)	132.1 (48-274.2)	7 (4.1-14.2)
Mesenchymal tumors	8.1 (2.5-18.3)	59.9 (3.8-121.6)	9.5 (4.5-49.6)

Table 2 Median percentage of blood vessels in tumor tissue (PctBVeTum), median percentage area of blood vessels in tumor tissue (PctAreaBVeTum), Median percentage of blood vessels in tumor stroma (PctBVeStrom) and median percentage area of blood vessels in tumor stroma (PctAreaBVeStrom) in dogs with epithelial tumors or mesenchymal tumors of the head, and corresponding *P*-values (* = statistically significant)

	Median PctBVeTum	Median PctAreaBVeTum	Median PctBVeStrom	Median PctAreaBVeStrom
Epithelial tumors	2.3% (0.4-4.5)	2.8% (0.6-4.1)	11.2% (5.2-22.6)	12% (4.7-22)
Mesenchymal tumors	4.4% (0.8-17.3)	4.4% (0.8-17.3)	13.2% (9.1-18.6)	14.4% (9.4-18.5)
P-values	0.06	0.04*	0.83	0.72

Table 3 *P*-values of multiple regression analysis assessing correlations between the tumor volume, the microvascular density and the dynamic contrast-enhanced computed-tomography perfusion parameters in a population of dogs with tumors of the head

Parameters	BV	BF	TT	Volume
PctBVeTum	0.55	0.58	0.60	0.83
PctAreaBVeTum	0.70	0.46	0.48	0.76
PctBVeStrom	0.78	0.47	0.64	0.64
PctAreaBVeStrom	0.53	0.56	0.51	0.65

BV blood volume, *BF* blood flow, *TT* transit time, *PctBVeTum* percentage of blood vessels in tumor tissue, *PctAreaBVeTum* percentage area of blood vessels in tumor tissue, *PctBVeStrom* percentage of blood vessels in tumor stroma, PctAreaBVeStrom: percentage area of blood vessels in tumor stroma

4.4% (0.5-17.6%), 4.4% (0.8-17.3%), 13.2% (9.1-18.6%), and 14.4% (9.4-18.5%).

Mesenchymal tumors had significantly higher PctAreaBVeTum than epithelial tumors ($P=0.04$). The other MVD parameters were not statistically different between epithelial and mesenchymal tumors (Table 2).

Association between tumor volume, perfusion parameters and MVD parameters

There was no significant association between tumor volume, perfusion parameters derived from DCECT and MVD parameters (Table 3).

Discussion

Mesenchymal tumors had a higher percentage area of blood vessels within the tumor tissue than epithelial tumors in our study. This seems in contrast with the greater BV and BF of epithelial tumors compared to mesenchymal tumors on DCECT. However, DCECT perfusion parameters were calculated on the entire mass, including stromal and tumoral tissue, and does not reflect specifically the percentage area of blood vessel within tumoral tissue. Epithelial tumors in our study were generally smaller than the mesenchymal tumors (median sizes 108.3 cm^3 and 150.8 cm^3, respectively), and large tumors can develop areas of hypoperfusion, necrosis, or cavitation that could have decreased their overall perfusion. However, correlation between tumor size and perfusion parameters has been inconsistent in human literature, as numerous interconnected environmental factors play a role in tumor perfusion, such as interstitial fluid pressure, growth rate, neoangiogenesis, and microvascular density, amongst others [29]. Although only the percentage area of blood vessels within the tumor tissue was significantly different between epithelial and mesenchymal tumors, the MVD parameters of mesenchymal tumors were all higher than those of epithelial tumors in our study (Table 2).

Previous studies showed that epithelial tumors had higher perfusion parameters than mesenchymal tumors. The first one included 31 dogs with spontaneous tumors (15 carcinomas and 16 sarcomas of various origins and sites) and showed that carcinomas had higher BF than soft tissue sarcomas. However, bone sarcoma had higher BF than soft tissue sarcoma in their study [20]. A second study assessed the perfusion parameters in 9 dogs with nasal tumors. Only 1 dog had a sarcoma but interestingly, this dog showed the lowest tumor perfusion parameters [30]. Finally, two recent papers assessed the DCECT perfusion parameters in dogs with nasal tumors and oro-facial tumors, respectively, and also found that carcinomas had higher BF and BV than sarcomas [21, 22]. They did not find any association between perfusion parameters and survival in the population of dogs with nasal tumors, but treatments and tumor types were very variable in this population, which could have biased the results [21]. In human medicine, perfusion parameters of carcinomas and sarcomas are not classically compared, yet soft tissue sarcomas seem to have lower perfusion parameters than carcinomas as well [31, 32].

This discrepancy of results between DCECT perfusion parameters and MVD in mesenchymal and epithelial tumors suggests that the number of blood vessels and tumor perfusion might be poorly correlated. One hypothesis is that blood vessels in sarcomas might have more structural and functional abnormalities than in carcinomas, resulting in reduced blood flow. Other parameters of the tumor microenvironment such as interstitial pressure might also play a role in the overall tumor perfusion [33]. Alternately, this could also be because the

pathological evaluation was done on a single tissue section, particularly small in case of endoscopy-guided tissue samples, that might not be representative of the whole tumor and for which the site of biopsy might not correspond to the volume included in the perfusion analysis.

Multiple studies in human medicine tried to correlate DCECT perfusion parameters and MVD and yielded inconsistent results, but several studies found positive correlations between BV, BF or both with MVD. This was the case in pancreatic tumors, prostatic tumors, adrenal tumors, head and neck squamous cell carcinomas, colorectal tumors, and soft tissue sarcomas [23–25, 34–39]. Only one study found a positive correlation between TT and MVD, and the authors hypothesized that morphologically abnormal, leaky, and loopy vessels could explain this correlation [21].

High MVD has been correlated to better radiosensitivity and better local tumor control in humans with head and neck carcinomas [3, 4, 10]. In veterinary medicine, high MVD was associated with higher occurrence of lymph node metastasis and malignancy in canine mammary tumors [5, 8]. Microvascular density was also higher in poorly differentiated than in well-differentiated squamous cell carcinomas of the skin in dogs, and canine cutaneous mast cell tumors with high MVD were more invasive, had a higher mitotic index and were associated with shorter survival times [6, 7]. We could not assess the MVD as a prognostic indicator in our study, due to the high variability in tumor types, localization and treatments.

Our study has several limitations. The number of dogs included was small, and tumor types and sites were varied. Some samples were relatively small biopsies whose vascular density may not reflect the overall tumor vascularity. It is the authors' experience that there's considerable variation in the histological vascularity of different subtypes of oral and nasal mesenchymal and epithelial tumors. For example, biopsies of chondrosarcomas are largely avascular as they consist mainly of cartilaginous matrix and neoplastic cells with little surrounding connective tissue whereas fibrosarcomas are far more vascular within biopsy specimens. This likely accounts for the large variation in vascularity as detected by histology. A similar pattern is observed for epithelial tumors with nasal adenocarcinomas, with exophytic growth into the nasal lumen, being sparsely vascular whereas squamous cell carcinomas which invade the lamina propria and establish a desmoplastic response are much more vascular. This microscopic view might not reflect the gross view established by imaging which would take into consideration wider changes in vascularization. For example, areas of chondrosarcoma may elicit an increased vascularization in adjacent tissue which would not be visible on histologic sections that are dominated by tumor tissue.

Some dogs received anti-inflammatory medications before DCECT, and their anti-COX-2 activity could alter the perfusion parameters [40].

Intra and inter-observer variability have not been calculated in this study but would have been interesting, especially since it represents the highest contributor to overall variability in DCECT [41]. In the same study, patients' blood pressure was not found to have a significant impact on the perfusion analysis [41].

Finally, only the center of masses longer than 4 cm was included in the perfusion analysis, and the site of biopsy was not recorded for each dog. It is therefore possible that the tissue sample was taken outside the volume scanned with DCECT in some dogs. This is particularly true for nasal tumors, where endoscopy-guided biopsies are taken at the most rostral (or sometimes caudal) extremity of the tumor. However, most of the tumor tissue was included in the perfusion analysis in most dogs, as only 3 dogs had a tumor length greater than 6 cm.

Conclusions

The present study showed that epithelial tumors had lower percentage area of blood vessels determined histologically than mesenchymal tumors in dogs with head tumors. However, there was no correlations between the MVD and the perfusion parameters derived from DCECT. These results add to the scarce literature about functional imaging of tumors in dogs and pave the way for future understanding of canine tumor vascularization and perfusion and their implications on prognosis.

Abbreviations

ATH	Adiabatic approximation of the tissue homogeneity
BF	Blood flow
BV	Blood volume
CI	Confidence interval
COX-2	Cyclo-oxygenase-2
DAB	3,3′-Diaminobenzidine
DCECT	Dynamic contrast-enhanced computed tomography
IQR	Interquartile ranges
MVD	Microvascular density
NSAID	Non-steroidal anti-inflammatory drug
PctAreaBVeStrom	Percentage area of blood vessels in stroma
PctAreaBVeTum	Percentage area of blood vessels in tumor tissue
PctBVeStrom	Percentage of blood vessels cells in stroma
PctBVeTum	Percentage of blood vessels cells in tumor tissue
RT	Radiotherapy
SCC	Squamous cell carcinoma
TT	Transit time

Acknowledgements

Not applicable.

Authors' contributions

JM, PR, LR and VB designed the study method. JM performed the clinical data collection, image acquisition and perfusion analysis. PR and LR performed the

histopathological analysis. JM and VB performed the statistical analysis. JM and PR drafted the manuscript. JM, PR, LR and VB reviewed the manuscript.

Funding
The authors received a research grant from the university of Liège for this work (FSR 2018).

Availability of data and materials
No datasets were generated or analysed during the current study.

Declarations

Ethics approval and consent to participate
Owner consent allowing for diagnostic tests including DCECT was obtained before inclusion into the study. Ethics approval was granted by the Veterinary Research Ethics Committee of the University of Liverpool under the reference VREC560a.

Consent for publication
Not applicable.

Competing interests
LR is a member of the *Veterinary Oncology* Editorial Board.

Received: 28 March 2024 Accepted: 10 May 2024
Published online: 16 July 2024

References

1. Cray M, Selmic LE, Kindra C, Abrams B, Story A, Hovis K, et al. Analysis of risk factors associated with complications following mandibulectomy and maxillectomy in dogs. J Am Vet Med Assoc. 2021;259(3):265–74. https://doi.org/10.2460/javma.259.3.265.
2. Weeden AM, Degner DA. Surgical approaches to the nasal cavity and sinuses. Vety Clin North Am Small Anim Pract. 2016;46(4):719–33. https://doi.org/10.1016/j.cvsm.2016.02.004.
3. Kamijo T, Yokose T, Hasebe T, Yonou H, Sasaki S, Hayashi R, et al. Potential role of microvessel density in predicting radiosensitivity of T1and T2stage laryngeal squamous cell carcinoma treated with radiotherapy. Clin Cancer Res. 2000;6(8):3159–65.
4. Zhang SC, Miyamoto SI, Kamijo T, Hayashi R, Hasebe T, Ishii G, et al. Intratumor microvessel density in biopsy specimens predicts local response of hypopharyngeal cancer to radiotherapy. Jpn J Clin Oncol. 2003;33(12):613–9. https://doi.org/10.1093/jjco/hyg121.
5. Graham JC, Myers RK. The prognostic significance of angiogenesis in canine mammary tumors. J Vet intern med. 1999;13(5):416–8. https://doi.org/10.1111/j.1939-1676.1999.tb01456.x.
6. Maiolino P, Papparella S, Restucci B, De Vico G. Angiogenesis in squamous cell carcinomas of canine skin: an immunohistochemical and quantitative analysis. J Comp Pathol. 2001;125(2–3):117–21. https://doi.org/10.1053/jcpa.2001.0485.
7. Preziosi R, Sarli G, Paltrinieri M. Prognostic value of intramoral vessel density in cutaneous mast cell tumour of the dog. J Comp Pathol. 2004;130(2–3):143–51. https://doi.org/10.1016/j.jcpa.2003.10.003.
8. Restucci B, De Vico G, Maiolino P. Evaluation of angiogenesis in canine mammary tumors by quantitative platelet endothelial cell adhesion molecule immunohistochemistry. Vet Pathol. 2000;37(4):297–301. https://doi.org/10.1354/vp.37-4-297.
9. Coomber BL, Denton J, Sylvestre A, Kruth S. Blood vessel density in canine osteosarcoma. Can J Vet Res. 1998;62(3):199–204.
10. Alessandrini L, Astolfi L, Daloiso A, Sbaraglia M, Mondello T, Zanoletti E et al. Diagnostic, prognostic, and therapeutic role for angiogenesis markers in head and neck squamous cell carcinoma: a narrative review. Int J of Mol Sci. 2023;24(13).https://doi.org/10.3390/ijms241310733.
11. Perivoliotis K, Baloyiannis I, Samara AA, Koutoukoglou P, Ntellas P, Dadouli K, et al. Microvessel density in patients with gastrointestinal stromal tumors: a systematic review and meta-analysis. World J Methodol. 2023;13(3):153–65.
12. Abbasi A, Ghaffarizadeh F, Mojdeganlou H. Prognostic significance of microvessel density in invasive ductal carcinoma of breast. Int J Hematol-Oncol Stem Cell Res. 2023. Available from: https://publish.kne-publishing.com/index.php/IJHOSCR/article/view/12646.
13. Saggioro M, D'Angelo E, Bisogno G, Agostini M, Pozzobon M. Carcinoma and sarcoma microenvironment at a glance: where we are. Front Oncol. 2020;10(March):1–9. https://doi.org/10.3389/fonc.2020.00076.
14. Morgan MJ, Lurie DM, Villamil AJ. Evaluation of tumor volume reduction of nasal carcinomas versus sarcomas in dogs treated with definitive fractionated megavoltage radiation: 15 cases (2010–2016). BMC Res Notes. 2018;11(1):1–6. https://doi.org/10.1186/s13104-018-3190-3.
15. Klotz E, Haberland U, Glatting G, Schoenberg SO, Fink C, Attenberger U, et al. Technical prerequisites and imaging protocols for CT perfusion imaging in oncology. Eur J Radiol. 2015;84(12):2359–67. https://doi.org/10.1016/j.ejrad.2015.06.010.
16. Razek AAKA, Tawfik AM, Elsorogy LGA, Soliman NY. Perfusion CT of head and neck cancer. Eur J Radiol. 2014;83(3):537–44. https://doi.org/10.1016/j.ejrad.2013.12.008.
17. Preda L, Calloni SF, Moscatelli MEM, Cossu Rocca M, Bellomi M. Role of CT perfusion in monitoring and prediction of response to therapy of head and neck squamous cell carcinoma. Biomed Res Int. 2014;2014:917150. https://doi.org/10.1155/2014/917150.
18. Petralia G, Bonello L, Viotti S, Preda L, D'Andrea G, Bellomi M. CT perfusion in oncology: how to do it. Cancer Imaging. 2010;10(1):8–19. https://doi.org/10.1102/1470-7330.2010.0001.
19. Troeltzsch D, Niehues SM, Fluegge T, Neckel N, Heiland M, Hamm B, et al. The diagnostic performance of perfusion CT in the detection of local tumor recurrence in head and neck cancer. Hiebl B, Krüger-Genge A, Jung F, eds. Clin Hemorheol Microcirc. 2020;76(2):171–7. https://doi.org/10.3233/CH-209209.
20. Nitzl D, Ohlerth S, Mueller-Schwandt F, Angst A, Roos M, Kaser-Hotz B. Dynamic computed tomography to measure tissue perfusion in spontaneous canine tumors. Vet Radiol Ultrasound. 2009;50(4):347–52. https://doi.org/10.1111/j.1740-8261.2009.01548.x.
21. Mortier JR, Maddox TW, Blackwood L, La Fontaine MD, Busoni V. Dynamic contrast-enhanced computed tomography in dogs with nasal tumors. J Vet Intern Med. 2023;37(3):1146–54. https://doi.org/10.1111/jvim.16722.
22. Mortier JR, Maddox TW, Blackwood L, La Fontaine MD, Busoni V. Dynamic contrast-enhanced computed tomography in 11 dogs with orofacial tumors. Am J Vet Res. 2023;7:lv–7. https://doi.org/10.2460/ajvr.22.12.0207.
23. Osimani M, Bellini D, Di Cristofano C, Palleschi G, Petrozza V, Carbone A, et al. Perfusion MDCT of prostate cancer: correlation of perfusion CT parameters and immunohistochemical markers of angiogenesis. Am J Roentgen. 2012;199(5):1042–8. https://doi.org/10.2214/AJR.11.8267.
24. d'Assignies G, Couvelard A, Bahrami S, et al. Pancreatic endocrine tumors: tumor blood flow assessed with perfusion CT reflects angiogenesis and correlates with prognostic factors. Radiology. 2009;250(2):407–16. https://doi.org/10.1148/radiol.2501080291.
25. Mayer P, Fritz F, Koell M, Vullierme MP, Hammel P, Hentic O, et al. Assessment of tissue perfusion of pancreatic cancer as potential imaging biomarker by means of Intravoxel incoherent motion MRI and CT perfusion: correlation with histological microvessel density as ground truth. Cancer Imaging. 2021;21(1):1–12. https://doi.org/10.1186/s40644-021-00382-x.
26. Bankhead P, Loughrey MB, Fernández JA, Dombrovski Y, McArt DG, Dunne PD, et al. QuPath: open source software for digital pathology image analysis. Sci Rep. 2017;7(1):1–7. https://doi.org/10.1038/s41598-017-17204-5.
27. McKinney W. Data structures for statistical computing in python. In: Proceedings of the 9th Python in Science Conference. Vol 1. 2010. p. 56–61.https://doi.org/10.25080/Majora-92bf1922-00a.
28. La Fontaine MD. The viability of DCE-CT kinetic analysis in tumor vasculature imaging in veterinary medicine. 2014.https://api.semanticscholar.org/CorpusID:74233549.
29. Aoki M, Takai Y, Narita Y, et al. Correlation between tumor size and blood volume in lung tumors: a prospective study on dual-energy gemstone spectral CT imaging. J Radiat Res. 2014;55:917–23. https://doi.org/10.1093/jrr/rru026.
30. Camp S, Fisher P, Thrall DE. Dynamic ct measurement of contrast medium washin kinetics in canine nasal tumors. Vet Radiol Ultrasound. 2000;41(5):403–8. https://doi.org/10.1111/j.1740-8261.2000.tb01861.x.
31. Trojanowska A, Trojanowski P, Bisdas S, Staskiewicz G, Drop A, Klatka J, et al. Squamous cell cancer of hypopharynx and larynx - Evaluation of

metastatic nodal disease based on computed tomography perfusion studies. Eur J Radiol. 2012;81(5):1034–9. https://doi.org/10.1016/j.ejrad.2011.01.084.
32. Tian F, Hayano K, Kambadakone AR, Sahani DV. Response assessment to neoadjuvant therapy in soft tissue sarcomas: using CT texture analysis in comparison to tumor size, density, and perfusion. Abdom Imaging. 2015;40(6):1705–12. https://doi.org/10.1007/s00261-014-0318-3.
33. Vaupel P. Tumor microenvironmental physiology and its implications for radiation oncology. Semin Radiat Oncol. 2004;14(3):198–206. https://doi.org/10.1016/j.semradonc.2004.04.008.
34. Ash L, Teknos TN, Gandhi D, Patel S, Mukherji SK. Head and neck squamous cell carcinoma: CT perfusion can help noninvasively predict intratumoral microvessel density. Radiology. 2009;251(2):422–8. https://doi.org/10.1148/radiol.2512080743.
35. Luczynska E, Gasinska A, Blecharz P, Stelmach A, Jereczek-Fossa BA, Reinfuss M. Value of perfusion CT parameters, microvessl density and VEGF expression in differentiation of benign and malignant prostate tumours. Pol J Pathol. 2014;3(3):229–36. https://doi.org/10.5114/pjp.2014.45787.
36. Qin HY, Sun H, Wang X, Bai R, Li Y, Zhao J. Correlation between ct perfusion parameters and microvessel density and vascular endothelial growth factor in adrenal tumors. PLoS ONE. 2013;8(11):1–9. https://doi.org/10.1371/journal.pone.0079911.
37. Goh V, Halligan S, Daley F, Wellsted DM, Guenther T, Bartram CI. Colorectal tumor vascularity: quantitative assessment with multidetector CT—Do tumor perfusion measurements reflect angiogenesis? Radiology. 2008;249(2):510–7. https://doi.org/10.1148/radiol.2492071365.
38. Kambadakone A, Yoon SS, Kim TMM, Karl DL, Duda DG, DeLaney TF, et al. CT perfusion as an imaging biomarker in monitoring response to neoadjuvant bevacizumab and radiation in soft-tissue sarcomas: comparison with tumor morphology, circulating and tumor biomarkers, and gene expression. Am J Roentgenol. 2015;204(1):W11–8. https://doi.org/10.2214/AJR.13.12412.
39. Zhou W, Wang X. The role of preoperative CT perfusion imaging in assessing colorectal cancer angiogenesis and its clinical value. Altern Ther Health Med. 2024:AT9520. Available from: http://europepmc.org/abstract/MED/38466054.
40. Mander K, Finnie J. Tumour angiogenesis, anti-angiogenic therapy and chemotherapeutic resistance. Aust Vet J. 2018;96(10):371-8. https://doi.org/10.1111/avj.12747.
41. La Fontaine MD, McDaniel LS, Kubicek LN, Chappell RJ, Forrest LJ, Jeraj R. Patient characteristics influencing the variability of distributed parameter-based models in DCE-CT kinetic analysis. Vet Comp Oncol. 2017;15(1):105–17. https://doi.org/10.1111/vco.12143.

Publisher's Note